



Multiple and Long-Term Disturbance of Gob-Side Entry Retaining by Grouped Roof Collapse and an Innovative Adaptive Technology

Changliang Han¹ · Nong Zhang¹ · Junhua Xue² · Jianguang Kan¹ · Yiming Zhao¹

Received: 16 March 2018 / Accepted: 25 September 2018 / Published online: 3 October 2018
© Springer-Verlag GmbH Austria, part of Springer Nature 2018

Abstract

The demand for gob-side entry retaining (GSER) technology is extensive in Chinese coal mines because of its outstanding advantages. However, due to the occurrence of long-term roof movement disturbances, maintaining the conventional GSER over long distances is difficult. The urgent demand for this technology and its difficult maintenance are prominent contradictions faced in its application. In this paper, two characteristics of strata movement after mining that have great influence on GSER are determined in a physical simulation experiment. One is that the roof layers, which are dominated by the key strata (KS), collapse in multiple groups to form two-directional periodic pressures and superposed disturbances. The other is that the movement of the main roof will experience three stages of deformation, as follows: bending subsidence before collapse, sinking deformation at collapse and compressive deformation after collapse. In particular, the gradual compression of the bulging gangue in the gob extends the disturbance cycle. Therefore, it is difficult to maintain the GSER over long distances because of the long-term and multiple breaking disturbances of the roof layers. Mechanical models of KS breaking and GSER are established, and a method to determine the timing and strength of KS disturbances are proposed. Making use of the characteristics of staged collapse and fluctuating weighting of the overlying strata, an innovative technology named short-staged GSER is proposed. This technology maintains the maximum length of GSER within the optimal length, which ensures that the entry avoids superposed disturbances, and reduces the maintenance difficulty. The method for determining the key technical parameters is discussed, and an engineering case in panel 24202 of the Shaqu Mine in China is presented. From a back-calculation of measurements, the engineering practice demonstrates that the surrounding rock mass is stable, and the deformed entry size is safe when the length of the short-staged GSER does not exceed 100 m.

Keywords Multiple disturbance · Gob-side entry retaining · Grouped roofs collapse · Surrounding rock

List of Symbols

a	The width of the GSER	E_1	The elastic modulus of the first layer
b	The width of the filling wall	E_2	The equivalent elastic modulus after mining injury of the immediate roof
E	The equivalent elastic modulus after mining injury of the coal seam	E_i	The elastic modulus of the i -layer
E_0	The equivalent elastic modulus after mining injury of the immediate floor	h_1	The height of the first layer
		h_i	The height of the i -layer
		h_0	The thicknesses of the immediate floor
		h	The thicknesses of the coal seam
		h_2	The thicknesses of the immediate roof
		H_0	The vertical distance between the KS and the coal seam
		h_k	The thickness of the KS
		K	The residual bulking coefficient of the immediate roof
		L_k	The length of the KS when it breaks
		L_m	The mining distance when the KS breaks
		L	The length of the sloping block of the main roof
		q	The load on the KS

✉ Changliang Han
hclayor@126.com

✉ Nong Zhang
zhangnong@cumt.edu.cn

¹ School of Mines, Key Laboratory of Deep Coal Resource Mining, Ministry of Education, China University of Mining and Technology, No. 1 Daxue Road, Xuzhou 221116, Jiangsu, China

² State Key Laboratory of Deep Coal Mining and Environment Protection, Huainan 232001, Anhui, China

$(q_n)_1$	The load formed by the n -layers on the first layer
s'	The deformation of the outside of the filling wall
s_p	The deformation of the main roof prior to collapse
s_c	The deformation of the main roof at collapse
s_a	The deformation of the main roof after collapse
s	The total deformation of the main roof
x_0	The horizontal distance from the breaking point of the main roof to the entry
α	The caving angle of the roof
δ	The space height from the filling wall to the immediate roof
σ_t	The tensile strength of the KS
σ_b	The largest load in the filling wall
γ_i	The volume force of the i -layer

1 Introduction

Gob-side entry retaining (GSER), which is retained along a gob by one filling body during the mining period of a longwall face, is a special type of entry that is substantially affected by the mining activity during construction (Zhang et al. 2016). Controlling the surrounding rock of a GSER structure is one of the most difficult support problems in a coal mine (Bai et al. 2015; Wang et al. 2015), in which rock mechanics issues, such as overburden movement (Cao and Zhou 2015), mining stress transfer and fracture instability of the rock mass (Kan et al. 2013; Li et al. 2016a), are encountered.

The demand for GSER in China's increasingly complex coal mining conditions is increasing due to the outstanding advantages of GSER, such as improvements in the coal recovery rate (Wang et al. 2016), reductions in the roadway drivage rate, and the realization of simultaneous coal and gas extraction (Yan et al. 2013; Zhang et al. 2012), mining, and depressurized mining (Li et al. 2016b) in a coal seam group. The contradiction between the technical demand for and the difficulty in support is the main contradiction in the application of GSER.

Many cases of GSER application exist in shallow coal seams with optimal mining conditions (Yang et al. 2015). However, GSER can be successfully employed twice in deep coal mines with large mining heights or long distances. More than half of the entries are damaged and destabilized by excessive deformation after 200 m and need to be repaired by machines before continued use (Zhang et al. 2014). The machine operation in GSER with high concentrations of gas and coal dust is very risky, as the entry is primarily used for air return. This phenomenon indicates that using GSER over long distances affects its normal use in many cases.

Many studies have attempted to innovate GSER technology; the research directions include the following: (1) a new

method for constructing an entry (Jiang et al. 2017; Zhang et al. 2015). One type of GSER without an artificial filling wall (He et al. 2017), which involves filling by a fracturing roof, was proposed. (2) New technology to support entry (Ma and Chen 2017; Ning et al. 2017; Ram et al. 2017). A strong and high-prestressed anchor is effective in the basic support of deep GSER (Kang et al. 2010). Drilling blasting technology is applied in the condition of a hard immediate roof (Han et al. 2015; Huang et al. 2017, 2018; Zhang et al. 2017), which provides a suitable stress environment after pressure relief. (3) New technology for a filling wall (Luan et al. 2018). A soft-hard backfill wall is proposed for a gob-side roadway (Tan et al. 2015; Wang et al. 2011); the bearing effect is better than the bearing effect for a common hard backfill wall. A GSER structure is simultaneously constructed using a fully mechanized gangue backfilling mining method (Gong et al. 2017). These studies are very useful in the popular applications of GSER. However, long-term roof collapse disturbance at the entry is unavoidable, and controlling the surrounding rock for GSER is still difficult.

In this study, an innovative technology for GSER is proposed based on the staged collapse characteristics and the long-term subsidence of the overlying strata above a gob, and an engineering case is presented. This technology provides a new method for resolving the contradiction between the technical requirements and the support difficulty.

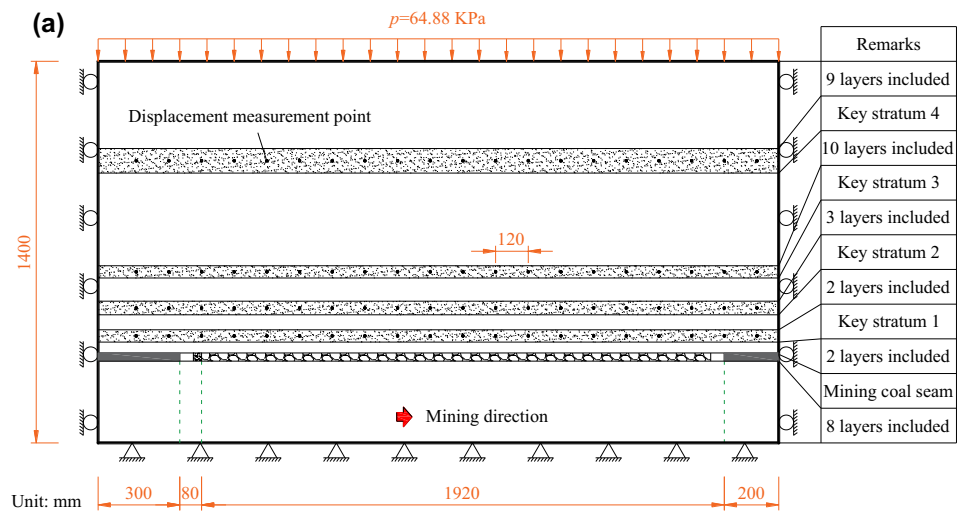
2 Staged Collapse of the Overlying Strata Above a Gob and Its Long-Term Disturbance to the Entry

2.1 Physical Simulation Scheme and Experimental Method

Understanding the movement of the overlying strata can help determine the GSER's disturbance source (Islavath et al. 2016; Salmi et al. 2017). One physical simulation experiment scheme was designed as a plane stress model, as shown in Fig. 1. Its boundary conditions were as follows: horizontal displacement constraints on the left and right boundaries, displacement constraint on the bottom boundary, and stress applied to the top boundary with a water bag.

The width, height and thickness of the model are 2.5 m, 1.4 m and 0.2 m, respectively, and the width and height of the simulated rock mass are 250 m and 140 m, respectively, with a geometric similarity ratio of 100:1. The model contains 39 strata, including 4 key strata (KS). Each stratum is formed by mixing sand, calcium carbonate and gypsum with different proportions, and mica powder is used to simulate the stratification. The surface of the model is painted white to improve identification. One displacement measuring line

Fig. 1 Experimental scheme and model. **a** Experimental scheme; **b** experimental model



is set for every KS, which are located 7 m, 17 m, 30 m and 70 m above the coal seam.

In the experiment, the mining height is 3 m, and the mining distance is 192 m. The coal seam is mined from left to right and is excavated every 5–10 m. Then, excavation continues after 5–30 min. During excavation, a three-dimensional photogrammetric system was used to monitor the deformation of the four KS, and a digital camera was used to record the motion state of the strata.

2.2 Grouped Collapse of Roofs Above the Gob

The collapse process of the overlying strata during mining is illustrated in Fig. 2. The roof layers above the gob collapse from bottom to top, and each collapse causes a disturbance to the surrounding rock mass. When the mining distances are 40 m (Fig. 2a), 80 m (Fig. 2c), 90 m (Fig. 2d) and 120 m (Fig. 2f), the 1st KS to the 4th KS successively collapse,

and the fracture height continuously develops. When a KS breaks, several soft rock strata above the KS are fractured and subside to keep pace with the KS (Ju and Xu 2013). The immediate roof separates from the original layer to the gob after fracturing occurs and becomes a loose gangue to fill the gob, whereas the main roof and the strata above the main roof maintain structural contact with the lateral boundary, and a load is applied to the lower rock mass through the residual roof on the side of the gob. During the grouped roof collapse, the fracturing of each layer will cause a disturbance to the GSER.

A large separation space exists between the collapsed rock strata and the adjacent unbroken rock strata, which causes truncation of the roof stress and shunting to two sides of the separation space. As observed in Fig. 2b–e, the separation between the collapsed layers has closed or partially closed, whereas the separation between the collapsed rock layers and the unbroken rock layers has increased to

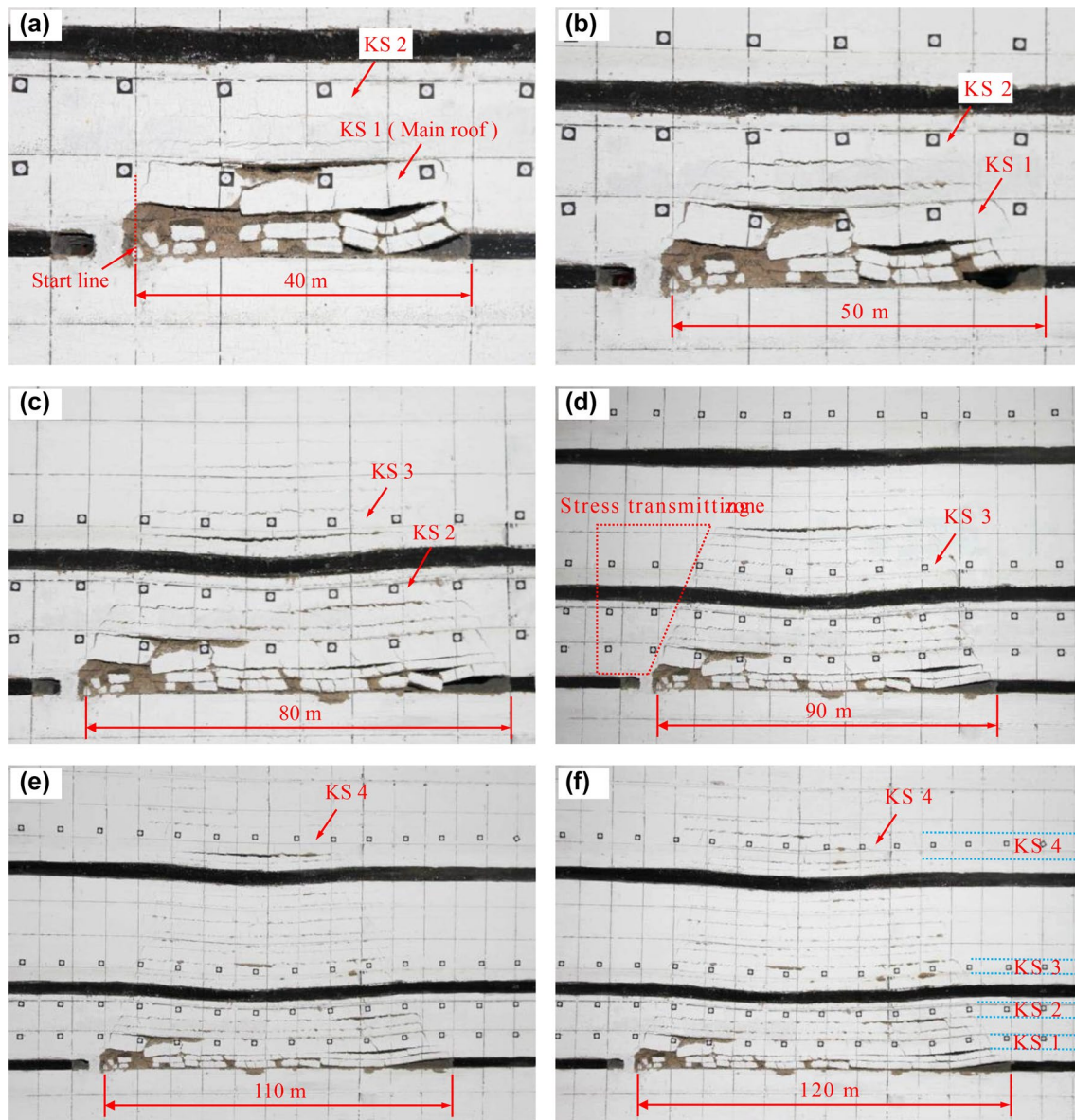


Fig. 2 Collapse process of the overlying strata during mining

its maximum. This space blocks the roof stress, which prevents it from directly moving downwards, and the roof stress moves downward through the trapezoidal rock mass on the lateral side of the gob (Fig. 2d). The GSER in this area will bear the stress.

2.3 Staged Subsidence of Roofs Above the Gob

The displacements of the four KS after each collapse are shown in Fig. 3. Every layer appears as a “V” shaped displacement after collapse, and the upper layers will exert stress on the lower layers and further compress the lower layers. When mining at 40 m, KS1 (the main roof) rotates and rapidly sinks after fracturing occurs; the maximum

subsidence is 2.10 m (Fig. 3a). Under the influence of the caving angle, the hanging distances of the other KS are smaller, and only a small deflection occurs. When mining at 80 m, KS2 fractures and sinks; the maximum subsidence is 2.27 m, which pressures KS1 to sink further (Fig. 3b). At this point, KS3 bears a heavy load due to the large number of overlying soft rock strata; thus, it also sinks but does not break down. When mining at 90 m, KS3 collapses with a maximum subsidence of 2.27 m (Fig. 3c). Similarly, the fracture of KS3 and the adjacent overlying strata promotes further deformation of the lower strata. When mining at 120 m, KS4 collapses with a maximum subsidence of 1.89 m (Fig. 3d), which is driven by the

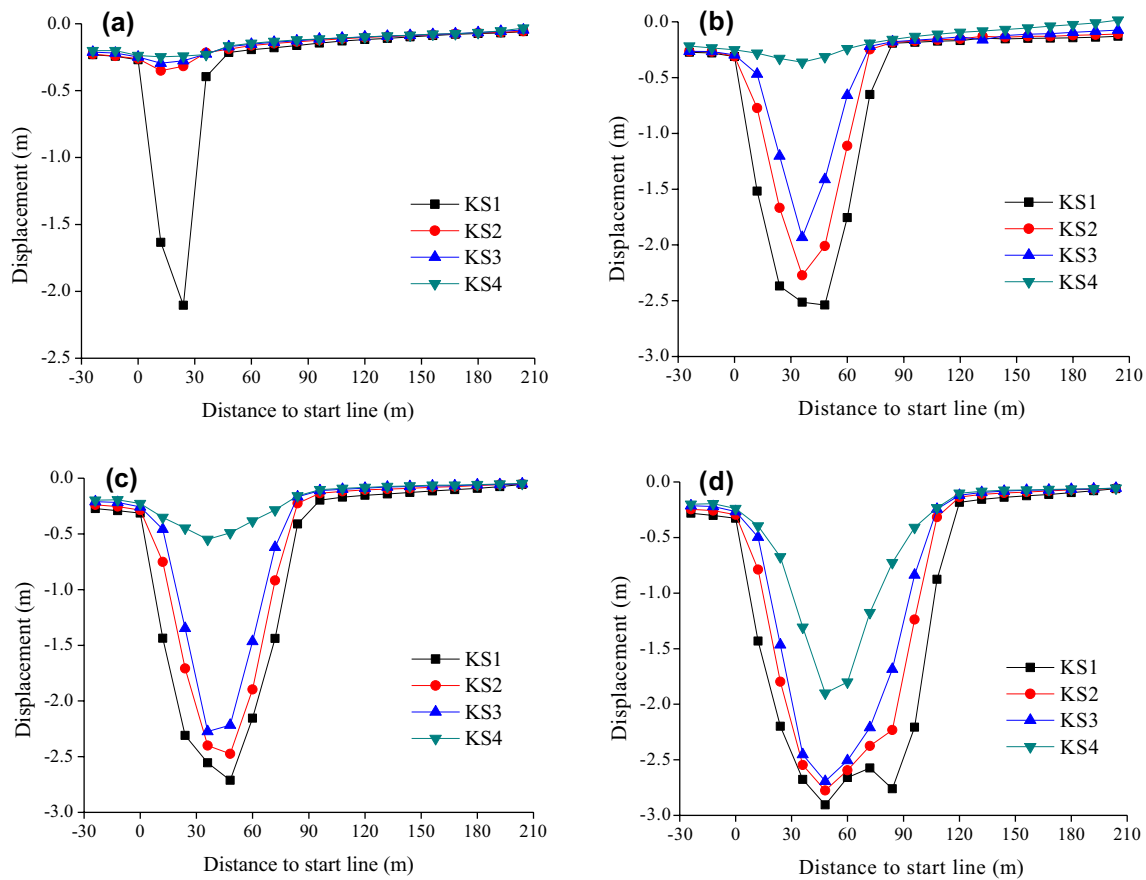


Fig. 3 Displacement of each stratum when one KS collapses: a KS1 collapse; b KS2 collapse; c KS3 collapse; and d KS4 collapse

large-scale overlying strata breaking off to compact the cavity in the unconsolidated waste rock.

The deformation of each KS consists of three stages: the bending deformation prior to collapse, the sinking deformation at collapse and the compressive deformation after collapse. The three stages of deformation differ at different heights, as shown in Fig. 4. The maximum subsidence for each of the four KS in the experiment are 3 m, 2.91 m, 2.85 m and 2.63 m. The three deformations of KS1, KS2, KS3, and KS4 are 14.7%, 55.4% and 29.9%; 32.8%, 45.2% and 22%; 67.9%, 12% and 20.1%; and 42.8%, 29.3% and 27.9%. The bending subsidence of the upper strata is significantly higher than that of the lower strata, whereas the instantaneous subsidence at collapse is significantly lower than that of the lower strata, which indicates that the upper strata are characterized by a “plastic beam”.

When one KS breaks, the subsidence continues, and further deformation occurs when the upper strata collapse. Considering KS1 as an example, Fig. 5a shows the displacement curve before and after the collapse of KS1, and Fig. 5b shows the change in the maximum subsidence of KS1 at each stage. As the first caving of the immediate roof has not been compacted and the KS1 subsidence is

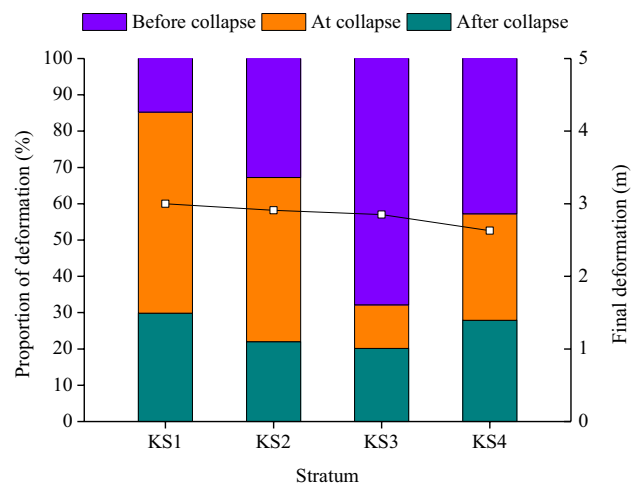


Fig. 4 Proportion of deformation for each KS

only 1.66 m at the moment of collapse, the maximum total subsidence is only 2.1 m. A subsidence of 0.9 m occurs after caving due to the compaction of loose waste rock in the gob.

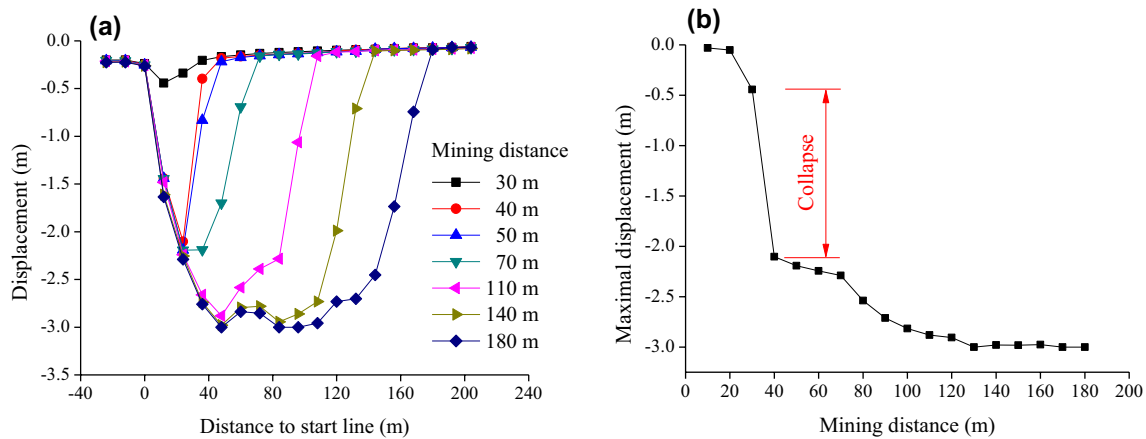


Fig. 5 Displacement of KS1 in different mining stages: **a** displacement before and after collapse; **b** maximum displacement of KS1

2.4 Disturbance Mechanism of GSER by Overlying Strata Movement

According to the experimental results, the movement state of the overlying strata is shown in Fig. 6. Roof fractures propagate both vertically and horizontally as mining progresses: the fractures in the same layer extend in the horizontal direction, and the fractures of different layers extend in the vertical direction. The GSER is disturbed by these two fractures. The immediate roof expands after collapse, with a bulking coefficient of approximately 1.3–1.4, and is then compacted under the pressure of the collapsed rock mass. The main roof and the other strata are compacted under the pressure of the subsequent rock collapse. This cycle repeats until the pressure attains a certain value and the residual bulking coefficient of the collapsed rock mass attains its minimum; then, the overburden movement ends.

In the process of multiple roof fractures, the sloping block on the edge of the mined-out area sinks as the bulking gangue is compressed, which continues to exert pressure on the GSER and creates maintenance difficulties for GSER structures covering long distances. When multiple KS break at a certain time, a strong superposed disturbance will occur. The characteristics of the roof movement can be applied to serve the

GSER; the key is to determine the timing of the roof collapse and the strength of the disturbance.

To determine the timing of the roof collapse, a mechanical model of KS breaking is established and is shown in Fig. 7.

The KS is supported by the adjacent layers prior to the breakage; thus, it can be considered a fixed beam at both ends. According to the maximal tensile stress criterion, the location that bears the maximal tensile stress will break. At this point, the length of the KS is L_k , as follows:

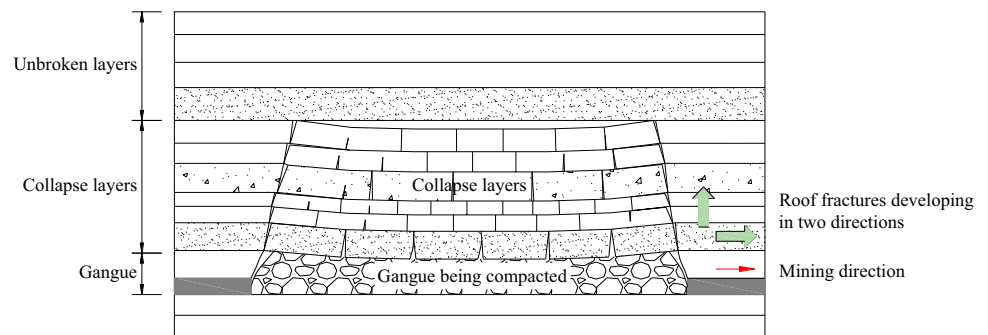
$$L_k = h_k \sqrt{\frac{2\sigma_t}{q}}, \tag{1}$$

where h_k and σ_t are the thickness of the KS and the tensile strength of the KS, respectively; q is the load on the KS, which can be calculated by Eq. (2) or Eq. (3).

As the KS controls the overlying strata, the curvature of each layer tends to be consistent. According to the principle of a composite beam, the load q of the KS is as follows:

$$(q_n)_1 = \frac{E_1 h_1^3 \sum_{i=1}^n \gamma_i h_i}{\sum_{i=1}^n E_i h_i^3}, \tag{2}$$

Fig. 6 Movement state of the slope overlying strata



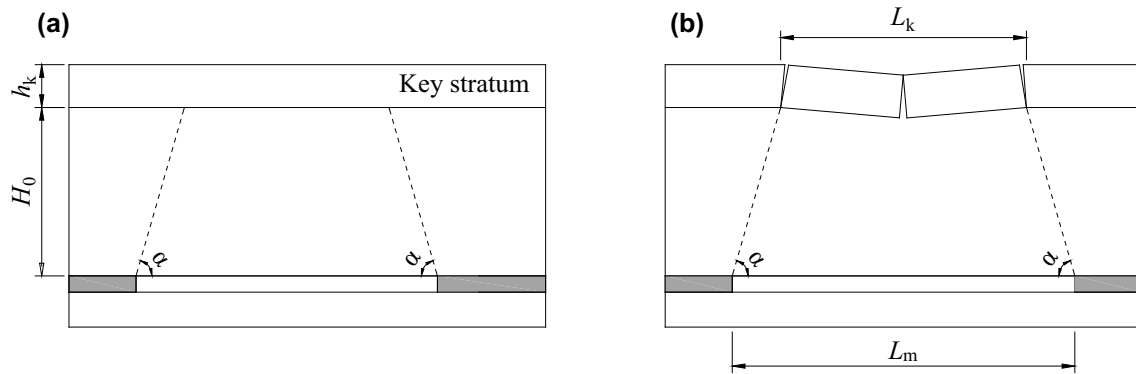


Fig. 7 Mechanical model of KS breaking: **a** before breaking; **b** after breaking

where $(q_n)_1$ is the load formed by the n -layers on the first layer; E_1 and h_1 are the elastic modulus and the height of the first layer; and γ_i , h_i and E_i are the volume force, height and elastic modulus, respectively, of the i -layer.

When the overlying strata above the KS are weak and fragile, the load q is as follows:

$$q = \sum_{i=1}^n \gamma_i h_i. \tag{3}$$

According to the geometrical relationship of the collapsed rock strata, the mining distance L_m when the KS breaks is expressed as follows:

$$L_m = h_k \sqrt{\frac{2\sigma_t}{q} + \frac{2H_0}{\tan \alpha}}, \tag{4}$$

where H_0 is the vertical distance between the KS and the coal seam, and α is the caving angle of the roof.

As shown in Eq. (4), the tensile strength, thickness, load, distance to the coal seam of the KS and the collapse angle of the roof affect the timing of the disturbance of the GSER structure.

To determine the roof weighting strength, the mechanical model of the surrounding rock structure of the GSER is shown in Fig. 8. In the figure, h_0 , h and h_2 are the thicknesses of the immediate floor, the coal seam and the immediate roof; x_0 is the horizontal distance from the breaking point of the main roof to the entry; a and b are the widths of GSER and the filling wall; δ is the space height from the filling wall to the immediate roof; L is the length of the sloping block of the main roof; s_p , s_c , and s_a are the deformation of the main roof prior to collapse, at collapse and after collapse, respectively; and s is the total deformation of the main roof.

The roof movement trend cannot be changed; according to the rule of “given deformation”, the position of

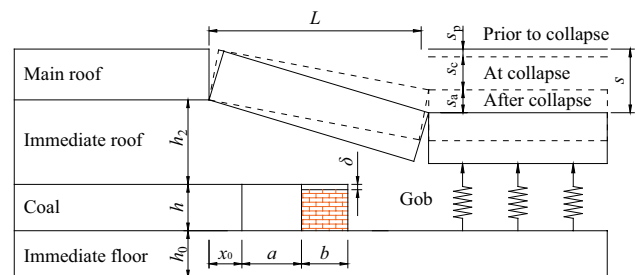


Fig. 8 Mechanical model of GSER

largest load bearing is the outside of the filling wall, and the stability of the location determines the total stability of the GSER.

K is the residual bulking coefficient of the immediate roof, as follows:

$$s = s_p + s_c + s_a = h - (K - 1)h_2. \tag{5}$$

The deformation of the outside of the filling wall s' is as follows:

$$s' = \frac{(x_0 + a + b)s}{L}. \tag{6}$$

E_0 , E and E_2 are the equivalent elastic modulus after the mining injury occurs. According to Hooke’s law, the largest load σ_b in the filling wall is expressed as follows:

$$\sigma_b = \frac{(x_0 + a + b)s - \delta L}{\left(\frac{h_0}{E_0} + \frac{h - \delta}{E} + \frac{h_2}{E_2}\right)L}. \tag{7}$$

The maximum weighting strength can be calculated by Eq. (7). The strength in each stage can be obtained by replacing the total subsidence of the main roof with the subsidence of each stage. When the maximum weighting strength of the wall is defined, the maximum allowable deformation can be calculated by Eq. (7).

3 Innovative Technology for Short-Staged GSER

3.1 Technology Concept

The grouped collapse of multiple strata over the gob will cause a superposed disturbance to the GSER. The longer the service time of the GSER is, the greater the disturbance time. Therefore, a large amount of deformation accumulates in a GSER that covers a long distance, which is prone to instability and may need to be repaired repeatedly. Repairing a GSER structure during the mining period is hazardous due to the high concentration of gas and coal dust.

The roof movement process of the gob is “sink–fracture–compaction–balance”, and the deformation of the GSER corresponds to the process characteristics of “slow

increase–rapid increase–decrease–stable”, as illustrated in Fig. 9. In the peak deformation stage, the entry is not only severely deformed but is also impacted by the roof and destroys the wall. If the construction of the GSER ends before the deformation reaches the allowable value, normal use of the entry can be ensured. Therefore, a GSER whose maximum length does not exceed the optimal length can avoid a series of problems caused by a large deformation.

Based on the characteristics of a staged collapse and the fluctuating weighting of the overlying strata, the layout of entries can be innovated for short-staged GSER, and the multi-breakage disturbance of the roof is averted.

3.2 Method for Short-Staged GSER

Figure 10 shows the construction method of a short-staged GSER. Three entries are arranged for the working face; two of these entries are arranged on the side of the GSER. Coal pillars are preserved between the two entries, and a crosscut is driven at intervals in the coal pillars. Fresh air exits from entry 1 and entry 2 through the short-staged GSER, crosscut and entry 3. During mining, the nearest crosscut at the back of the working face is opened, and this crosscut is used to return air. The remaining crosscuts are closed with wind walls. At the rear of the working face, the wall along the gob is filled; entry 2 forms a GSER. The maximum length of the short-staged GSER is the distance L_p between the crosscuts. When the GSER reaches the next crosscut, the closing wall in the crosscut is removed and opened. At the rear of the GSER and entry 3, closed walls will be built to seal them.

Prior to mining the adjacent working face, the closed wall in entry 2 and entry 3 are opened to repair the GSER that

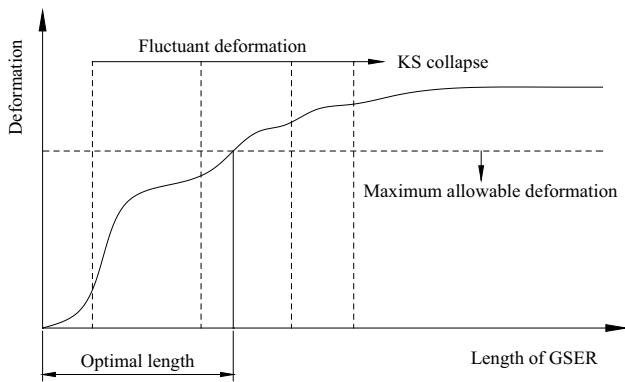
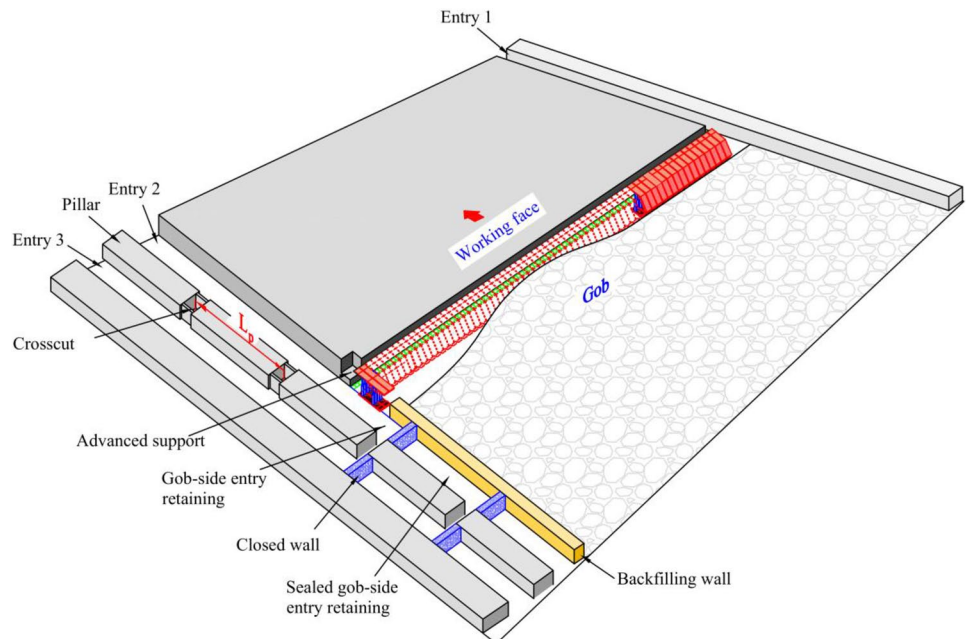


Fig. 9 Optimal length of GSER

Fig. 10 Short-staged GSER



has a large deformation. The GSER continues to service the next working face, whereas the coal pillar is mined as part of the working face.

3.3 Method for Determining Key Parameters

The timing of the disturbance to the GSER can be obtained when the limit span of each KS over the gob is determined. Based on the analysis of the roof structure, Eq. (1) is adopted to obtain the limit span of each KS, and then Eq. (4) is used to obtain the mining distance of the working face when the KS breaks. According to the mining distance, the disturbance time of the KS is known.

Determining the optimal length is the key to implementing a short-staged GSER to avoid instability caused by excessive deformation. The largest load on the filling wall, which is related to the roof displacement, can be calculated by Eq. (7). To ensure that the largest load on the filling wall does not exceed the maximum strength of the wall, the maximum allowable deformation of the roof can be back calculated. Then, the optimal length of a short-staged GSER is obtained, combining the formation characteristics of roof subsidence at different mining distances measured experimentally or in a field test.

4 Case Study

4.1 Geological and Engineering Conditions

The Shaqu mine is located in Lvliang City, Shanxi Province, China. Panel 24202 is designed to mine the #4 coal seam. The coal seam contains one of the world's best coking coal due to its low ash concentration, low sulphur concentration, low phosphorus concentration, medium volatility and excellent adhesion. This coal has the reputation of being a "Chinese coal treasure". The average height, dip angle and burial depth are 2.6 m, 4°, and 471 m, respectively. The maximum absolute gas emission rate of panel 24202 is 65 m³/min. The strata occurrence is shown in Table 1.

The width and length of panel 24202 are 210 m and 1030 m, respectively. Three roadways were designed as follows: two roadways with an air entry and one roadway with an air return entry. Crosscuts were set at 50 m intervals between the belt entry and the air return entry (see Fig. 11 for details). A belt entry was planned for the GSER; the entry was a rectangular section with a width of 4.2 m and a height of 2.8 m. A combination support mode with a rock bolt and an anchor cable was employed. The dimensions of the bolt and cable for the roof are $\Phi 22$ mm \times 2.4 m (density of 5/m) and $\Phi 17.8$ mm \times 7.3 m (density of 5/m), respectively. The bolt for the coal rib is $\Phi 22$ mm \times 2.4 m (density of 5/m).

Table 1 Strata occurrence in panel 24202

Accumulative thickness (m)	Thickness (m)	Lithology	Remarks
41.2	4.3	Mudstone	
36.9	15.5	Medium sandstone	KS3
21.4	2.1	Mudstone	
19.3	1.0	#2 Coal seam	
18.3	1.8	Mudstone	
16.5	1.6	Fine sandstone	
14.9	5.4	Medium sandstone	KS2
9.5	0.5	Mudstone	
9	2.1	Siltstone	
6.9	3.1	Fine sandstone	KS1
3.8	1.2	#3 Coal seam	
2.6	1.0	Mudstone	
1.6	0.8	Fine sandstone	
0.8	0.8	Mudstone	Immediate roof
0	2.6	#4 Coal seam	Coal seam mining
	3.7	Fine sandstone	Immediate floor

4.2 New GSER Scheme

Due to the high gas content of the coal seam in panel 24202, a GSER was provided in the belt entry during mining and along the working face to form a Y-type ventilation system. The Y-type ventilation system can resolve the problem of frequent over-limiting of gas in a traditional U-shaped ventilation system. In addition, the gas in the roof fracture zone and gob can be extracted by the space of the GSER. While ensuring the safety of the working face, coal and gas are mined to maximize the resource recovery.

The conventional GSER method is shown in Fig. 12a. During the mining period, belt entry will be provided for the GSER along the total length; however, the deformation of the entry will be gradually aggravated, and the cross-section will considerably decrease to satisfy the demand. In this manner, the rear entry needs to be repaired at the time of mining. However, the return air at the entry has a high gas concentration. A potential safety hazard exists in the repair work, which hinders balancing production with safety.

The new GSER scheme design is illustrated in Fig. 12b. Three entries were arranged on panel 24202. A short-staged GSER was to be conducted in the belt entry, and construction was expected to be completed before the entry reached the maximum deformation to ensure the stability of the surrounding rock. On the GSER side at the front of the working face, an area was extracted by a mining machine to support the roof. After the hydraulic support was pushed over, the gob-side filling was completed behind the working surface and under the supported roof. Prefabricated blocks were

Fig. 11 Entry layout of panel 24202

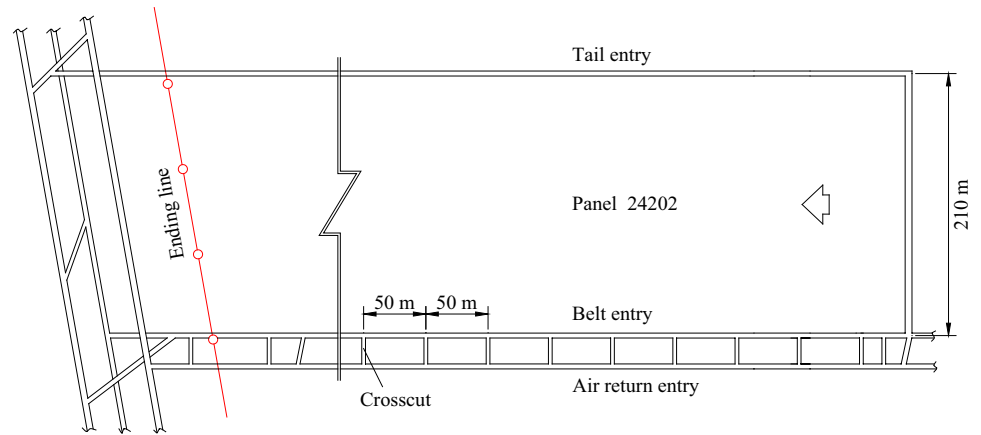
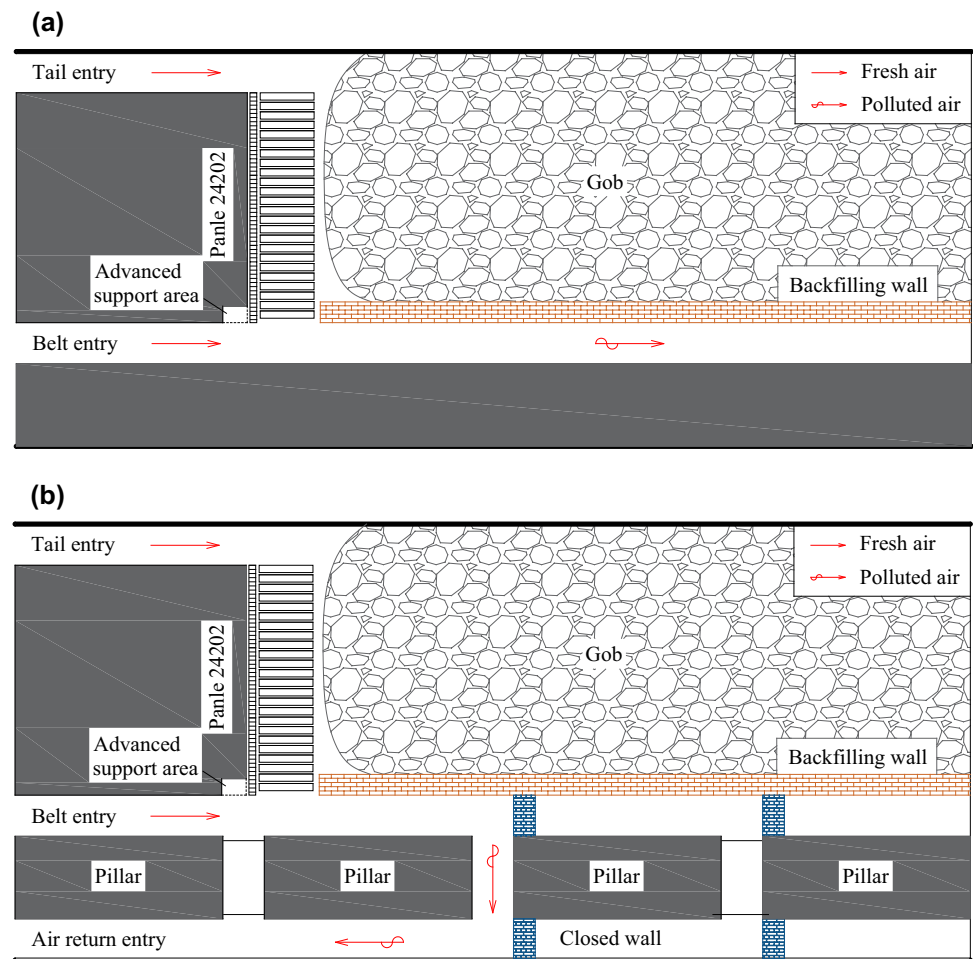


Fig. 12 Methods of GSER in panel 24202: **a** traditional method; **b** new method



piled into a wall. The blocks were constructed of cement, fly ash, sand, gravel and additives. The dimensions of the blocks were 800 mm × 180 mm × 120 mm. The blocks were cemented with a paste of cement and water. The width of the filling wall for the short-staged GSER was reduced to 1.6 m. Thus, the ratio of width-to-height was 0.57, which is lower than the value of 0.8–1.2 in conventional GSER structures.

Determining the length of the short-staged GSER is the key to ensuring the stability of the surrounding rock in the service time. The tensile strengths of KS1, KS2 and KS3 are 4.5 MPa, 6.3 MPa and 7.9 MPa, respectively. The volume force of the overlying strata is 0.025 MN/m³. The caving angle of the roof is 70°. The length of the KS1 fracture calculated by Eqs. (1) and (3) is 24.6 m. From Eq. (4), the

mining distance at fracture is 27.4 m. Similarly, the calculated fracture lengths for KS2 and KS3 are 36.6 m and 87.6 m, respectively, and the mining distances at fracture are 43.5 m and 103.2 m. The GSER will have been disturbed by three roof fractures before the mining distance reaches 105 m.

When $K=1.1$, the total subsidence value of the main roof is 2.2 m, according to Eq. (5). The strength of the filling wall is 30 MPa, and the maximum space height (δ) is 0.05 m. The actual measured $x_0=12$ m, $E_1=400$ MPa, $E=200$ MPa, and $E_2=320$ MPa. The roof deformation and wall load at different stages are back calculated by (7), as shown in Fig. 13. When the wall load is 30 MPa, the maximal allowable roof displacement is 1.5 m, and the mining distance is 110 m. When the roof displacement is 2.2 m, the load applied to the wall is 45.5 MPa, which substantially exceeds the maximum load of the wall. Therefore, the maximal length of the short-staged GSER is determined to be 110 m. Considering that the space between two crosscuts is 50 m, the length of the short-staged GSER is preferably 50 m or 100 m.

4.3 Analysis of Effect

To further ascertain the reasonable length, the maximal length of the GSER in the early stage of the test was 150 m. A cross-section method was used to monitor the deformation of the maximal displacement point in the middle of the four sides of the GSER, as shown in Fig. 14. In the first 20 m, the deformations of the roof–floor and rib–rib were within 0.15 m. During the period of 20–30 m, the deformations of the roof–floor and rib–rib were 0.4 m and 0.16 m, respectively. A deformation jump exists from 30 to 40 m. This deformation was caused by the breaking of KS1 and KS2. The deformation maintained a slow growth but fluctuated

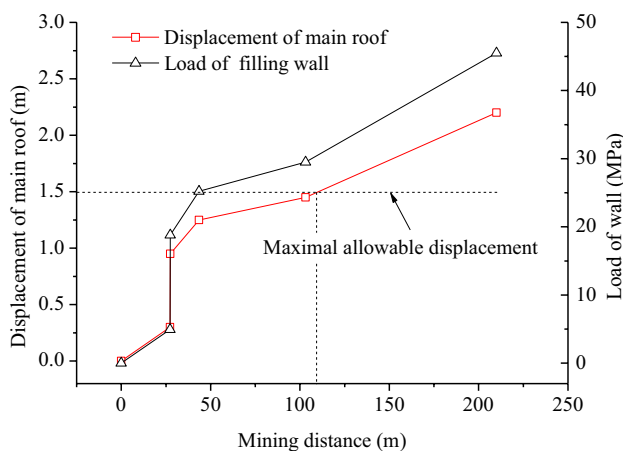


Fig. 13 The maximal length of the short-staged GSER determined by roof displacement and wall load

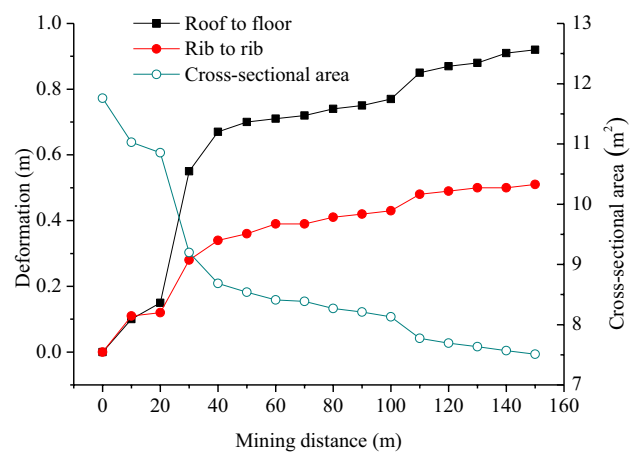


Fig. 14 Deformation of GSER in panel 24202

from 90 to 110 m, which was caused by the KS3 breaking disturbance.

Regarding the maintenance status, during the period of 0–60 m, the GSER deformed, but the stability of the surrounding rock was excellent. From 60 to 110 m, small cracks occurred in part of the wall, and a rupture gradually appeared in the ribs and floor. After 110 m, the rupture of the surrounding rock was more distinct, as follows: the coal body fractured and formed net bags, part of the rock bolts broke in the coal rib, the filling wall was significantly exfoliated, and the floor exhibited aggravated heave. When the length was 150 m, the deformations of the roof–floor and coal rib were 0.92 m and 0.51 m, respectively, and the section reduced from 11.76 to 7.51 m². The deformation of the GSER was not stable and exhibited an increasing trend.

According to the monitoring results, the optimal length of the short-staged GSER was 50 m, and the maximal length should not exceed 100 m, which is one or two times the horizontal distance between crosscuts. In a subsequent period, this scheme was implemented. The effective section of the short-staged GSER remained at a minimum area of 8.5 m² during mining, which satisfied the demand for use, and the phenomenon of instability occurred in the surrounding rock.

5 Conclusions

1. Roof fractures developing in two directions during the mining process: the fractures in the same layer extend in the horizontal direction, and the fractures of different layers extend in the vertical direction. Each fracture will cause a disturbance to the GSER, and the trapezoidal rock mass on the side of the gob area is the transmission path of the disturbance stress.
2. The deformation of each KS consists of three stages, as follows: the bending deformation prior to collapse,

the sinking deformation at collapse and the compressive deformation after collapse. The underside entry should be subjected to these three subsidence deformations. Due to the gradual compression of the bulging gangue in the gob, the KS will continue to sink after breaking, which will exert pressure on the GSER for an extended period of time and hinder the ability to maintain a GSER that covers a long distance.

3. A method for determining the timing of the roof collapse and the strength of the disturbance by the KS is obtained.
4. An innovative technology named short-staged GSER is proposed based on the characteristics of the staged collapse and the fluctuating weighting of the overlying strata. The GSER enables the entry to avoid multiple fracture disturbances and reduces the maintenance difficulty.
5. In the engineering application of panel 24202 of the Shaqu Mine in China, the reasonable distance for the short-staged GSER is determined to be 50 m, and the maximum distance is 100 m. The width-to-height ratio is 0.57, which is lower than the value of 0.8–1.2 obtained by the conventional GSER method. A narrow wall satisfies the bearing requirements. Total maintenance of the entry works well, which verifies the rationality of the new technology.

Acknowledgements This study was funded by the National Natural Science Foundation of China (Grant no. 51404251), the Natural Science Foundation of Jiangsu Province (Grant no. BK20140198), and the Priority Academic Program Development of Jiangsu Higher Education Institutions.

References

- Bai JB, Shen WL, Guo GL, Wang XY, Yu Y (2015) Roof deformation, failure characteristics, and preventive techniques of gob-side entry driving heading adjacent to the advancing working face. *Rock Mech Rock Eng* 48:2447–2458
- Cao ZZ, Zhou YJ (2015) Research on coal pillar width in roadway driving along goaf based on the stability of key block. *Comput Mater Contin* 48:77–90
- Gong P, Ma ZG, Zhang RRC, Ni XY, Liu F, Huang ZM (2017) Surrounding rock deformation mechanism and control technology for gob-side entry retaining with fully mechanized gangue backfilling mining: a case study. *Shock Vib* 2017:6085941
- Han CL, Zhang N, Li BY, Si GY, Zheng XG (2015) Pressure relief and structure stability mechanism of hard roof for gob-side entry retaining. *J Cent South Univ* 22:4445–4455
- He MC, Gao YB, Yang J, Gong WL (2017) An innovative approach for gob-side entry retaining in thick coal seam longwall mining. *Energies* 10:1785
- Huang BX, Chen SL, Zhao XL (2017) Hydraulic fracturing stress transfer methods to control the strong strata behaviours in gob-side gateroads of longwall mines. *Arab J Geosci* 10:236
- Huang BX, Liu JW, Zhang Q (2018) The reasonable breaking location of overhanging hard roof for directional hydraulic fracturing to control strong strata behaviors of gob-side entry. *Int J Rock Mech Min* 103:1–11
- Islavath SR, Deb D, Kumar H (2016) Numerical analysis of a longwall mining cycle and development of a composite longwall index. *Int J Rock Mech Min* 89:43–54
- Jiang LS, Zhang PP, Chen LJ, Hao Z, Sainoki A, Mitri HS, Wang QB (2017) Numerical approach for goaf-side entry layout and yield pillar design in fractured ground conditions. *Rock Mech Rock Eng* 50:3049–3071
- Ju J, Xu J (2013) Structural characteristics of key strata and strata behaviour of a fully mechanized longwall face with 7.0 m height chocks. *Int J Rock Mech Min* 58:46–54. <https://doi.org/10.1016/j.ijrmms.2012.09.006>
- Kan JG, Zhang N, Wu JK, Wu H (2013) Effect of main roofs fracture position on the secondary gob-side entry retaining stability. *Disaster Adv* 6:189–199
- Kang H, Niu D, Zhang Z, Lin J, Li Z, Fan M (2010) Deformation characteristics of surrounding rock and supporting technology of gob-side entry retaining in deep coal mine. *Chin J Rock Mech Eng* 29:1977–1987 (in Chinese)
- Li XH, Ju MH, Yao QL, Zhou J, Chong ZH (2016a) Numerical investigation of the effect of the location of critical rock block fracture on crack evolution in a gob-side filling wall. *Rock Mech Rock Eng* 49:1041–1058
- Li ZL, Dou LM, Cai W, Wang GF, Ding YL, Kong Y (2016b) Roadway stagger layout for effective control of gob-side rock bursts in the longwall mining of a thick coal seam. *Rock Mech Rock Eng* 49:621–629
- Luan HJ, Jiang YJ, Lin HL, Li GF (2018) Development of a new gob-side entry-retaining approach and its application. *Sustainability* 10:470
- Ma SQ, Chen Y (2017) Application of hydraulic fracturing and energy-absorption rockbolts to improve the stability of a gob-side roadway in a 10-m-thick coal seam: case study. *Int J Geomech* 17:05017002
- Ning JG, Wang J, Bu TT, Hu SC, Liu XS (2017) An innovative support structure for gob-side entry retention in steep coal seam mining. *Minerals* 7:75
- Ram S, Kumar D, Singh AK, Kumar A, Singh R (2017) Field and numerical modelling studies for an efficient placement of roof bolts as breaker line support. *Int J Rock Mech Min* 93:152–162. <https://doi.org/10.1016/j.ijrmms.2017.01.013>
- Salmi EF, Nazem M, Karakus M (2017) Numerical analysis of a large landslide induced by coal mining subsidence. *Eng Geol* 217:141–152
- Tan YL, Yu FH, Ning JG, Zhao TB (2015) Design and construction of entry retaining wall along a gob side under hard roof stratum. *Int J Rock Mech Min* 77:115–121
- Wang H, Zhang D, Fan G (2011) Structural effect of a soft–hard backfill wall in a gob-side roadway. *Min Sci Technol* 21:313–318. <https://doi.org/10.1016/j.mstc.2011.05.001>
- Wang M, Bai JB, Li WF, Wang XY, Cao SG (2015) Failure mechanism and control of deep gob-side entry. *Arab J Geosci* 8:9117–9131
- Wang HS, Zhang DS, Liu L, Guo WB, Fan GW, Song KI, Wang XF (2016) Stabilization of gob-side entry with an artificial side for sustaining mining work. *Sustainability* 8:627
- Yan S, Bai J, Wang X, Huo L (2013) An innovative approach for gateroad layout in highly gassy longwall top coal caving. *Int J Rock Mech Min* 59:33–41. <https://doi.org/10.1016/j.ijrmms.2012.11.007>
- Yang HY, Cao SG, Li Y, Sun CM, Guo P (2015) Soft roof failure mechanism and supporting method for gob-side entry retaining. *Minerals-Basel* 5:707–722

- Zhang N, Yuan L, Han CL, Xue JH, Kan JG (2012) Stability and deformation of surrounding rock in pillarless gob-side entry retaining. *Saf Sci* 50:593–599
- Zhang N, Zhang Z, Wu H, Cao P (2014) Technology and application of reparation in deep gob-side entry retaining. *Chin J Rock Mech Eng* 33:468–474 (in Chinese)
- Zhang ZZ, Bai JB, Chen Y, Yan S (2015) An innovative approach for gob-side entry retaining in highly gassy fully-mechanized long-wall top-coal caving. *Int J Rock Mech Min* 80:1–11
- Zhang ZY, Shimada H, Qian DY, Sasaoka T (2016) Application of the retained gob-side gateroad in a deep underground coalmine. *Int J Min Reclam Environ* 30:371–389
- Zhang ZY, Zhang N, Shimada H, Sasaoka T, Wahyudi S (2017) Optimization of hard roof structure over retained goaf-side gateroad by pre-split blasting technology. *Int J Rock Mech Min* 100:330–337

Publisher's Note Springer Nature remains neutral with regard to jurisdictional claims in published maps and institutional affiliations.